complexes show visible-region CT spectra typical of the ruthenium(II) component. In the solid state the complexes are intensely colored, have FTIR ν(CN) frequencies differing from the simple alkali-metal hexacyano anions, and presumably do involve some charge transfer under these conditions. A strong solution of the ferricyanide ion pair in aqueous solution shows a broad band centered about 15 150 (670) cm^{-1}. This is not present in either of the components and may be an intervalence transition.[33-35]

Acknowledgment. The authors are indebted to the Natural Sciences and Engineering Research Council of Canada for financial assistance through operating and strategic grants and for a Summer Studentship to G.E. We are also indebted to the Office of Naval Research, Washington, DC, for a joint grant in collaboration with Prof. A. J. Bard.

Registry No. $Ru(bpz)_3^{2+}$, 75523-96-5; $Fe(H_2O)_6^{3+}$, 15377-81-8; $Fe(H_2O)_6^{2+}$, 15365-81-8; $Cu(H_2O)_4^{2+}$, 22174-11-4; $[Fe(CN)_6]^{4-}$, 13408-63-4; $[Fe(CN)_6]^{3-}$, 13408-62-3; $[Co(NH_3)_6]^{3+}$, 14695-95-5; $[Co(NH_3)_5Cl]^{2+}$, 14970-14-0; $Co(H_2O)_6^{2+}$, 15276-47-8; $Mn(H_2O)_6^{2+}$, 15365-82-9; $Ru(bpz)_2(bpzH)^{3+}$, 95865-85-3; $Ru(bpzH_2)_3^{8+}$, 95865-86-4; Ag^I/NO_3^-, 7761-88-8; I^-, 20461-54-5; *N,N'*-diphenyl-*p*-phenylenediamine, 74-31-7; phenothiazine, 92-84-2; *N,N*-dimethyl-*p*-toluidine, 99-97-8; *N,N*-dimethylaniline, 121-69-7; diphenylamine, 122-39-4; aniline, 62-53-3; triphenylamine, 603-34-9; 1,2,4-trimethoxybenzene, 135-77-3; 1,4-dimethoxybenzene, 150-78-7; 1,2,3-trimethoxybenzene, 634-36-6; 1,2-dimethoxybenzene, 91-16-7; 1,3,5-trimethoxybenzene, 621-23-8.

Contribution from the Department of Chemistry, York University, Downsview, Toronto, Ontario, Canada M3J 1P3

Protonation and Lewis Acid-Lewis Base Equilibria in (Bipyrazine)molybdenum and (Bipyrazine)tungsten Tetracarbonyls

ELAINE S. DODSWORTH, A. B. P. LEVER,* GORAN ERYAVEC, and ROBERT J. CRUTCHLEY

Received July 30, 1984

The title complexes react with boron trifluoride etherate to generate mono- and diadducts of BF_3. In H_2SO_4/ethanol solution one proton is coordinated. In each case reaction is assumed to occur at the peripheral uncoordinated nitrogen atoms of the bipyrazine unit. New metal-to-ligand charge-transfer bands are observed for these various species. Analysis of the spectra shows that $pK_a(1)$ for the first uncoordinated nitrogen atom is about -0.3 (Mo complex) and that extensive mixing of ground and excited states must be occurring to account for the oscillator strengths and band widths observed.

Introduction

Ground- and excited-state protonation equilibria involving the $Ru(bpz)_3^{2+}$ ion (bpz = bipyrazine) have recently been reported.[1] This species binds up to six protons in a stepwise fashion, providing an interesting series of electronic absorption and emission data. Of special interest was the variation in metal-to-ligand charge-transfer (MLCT) energy as a function of the degree and site of protonation. Stepwise protonation provides a useful mechanism for "tuning" excited-state redox potentials[2] and is of obvious interest in the design of photocatalytic redox reagents. Previous studies of protonation equilibria involving inorganic complexes have discussed protonation at the nitrogen atom of coordinated cyanide ion in species such as $M(CN)_4L$ and $M(CN)_2L_2$ (M = Fe, Ru; L = diimine),[3,4] considered the enhanced acidity of ruthenium(II) complexes of 4,7-dihydroxy-1,10-phenanthroline[5], and analyzed the pH dependence of ruthenium bipyridine[6] and bipyrimidine[7] species. As is evident, much of the work has been associated with ruthenium or its congeners. The binding of Lewis acids to cyanide complexes and its effect on their charge-transfer spectra has also been studied.[8] For these reasons we considered it useful to probe the protonation equilibria in a complex other than ruthenium having only one bipyrazine unit to provide a data set that might be capable of more detailed analysis and additional insights.

The species $M(CO)_4(bpz)$ (M = Mo, W)[9] are soluble in organic solvents and give rise to intense absorption in the visible region, attributed to metal-to-ligand charge-transfer (MLCT) M → bpz(π^*). Addition of mineral acid, or the Lewis acid BF_3 (etherate) causes changes in the visible absorption spectra that can be interpreted in terms of mono- and diacid equilibria. FTIR and NMR data are reported in support of the equilibria proposed.

Table I. Electronic Spectra of $M(CO)_4bpz$ in the Presence of $Et_2O{\cdot}BF_3$[a]

approx concn of $Et_2O{\cdot}BF_3$, mol L^{-1}	color	λ_{max}, nm					
		$Mo(CO)_4bpz$			$W(CO)_4bpz$		
		II	I/Ib	Ia	II	I/Ib	Ia
0	pink	368.5	520		371	533	
0.07	pink	369	523	sh	371	534	sh
0.13	mauve	370	527	618	371	539	616
0.17	blue	371	sh	625	371	sh	620
0.20	blue	371	494	640	sh	482	630
0.33	gray-blue	sh	490	653	...	480	640
7.9[b]	gray-blue				322	490	654

[a] Spectra recorded using approximately 10^{-4} M $M(CO)_4bpz$ in acetone. Solutions were deoxygenated with dry N_2 before addition of $Et_2O{\cdot}BF_3$. [b] Complex dissolved in pure $Et_2O{\cdot}BF_3$.

Experimental Section

The complexes $Mo(CO)_4(bpz)$ and $W(CO)_4(bpz)$ were prepared according to literature methods.[9] Acetone and 96% H_2SO_4 were BDH Analar grade. The acid was diluted with absolute ethanol. Boron trifluoride etherate was purified according to a literature method[10] and stored under nitrogen or dry air. Electronic spectra were recorded on a Perkin-Elmer Hitachi Model 340 microprocessor spectrophotometer. The cell holder was cooled to ca. 10 °C to minimize decomposition of the complexes. ^1H NMR spectra were recorded on a Varian EM360 60 MHz spectrometer at ambient temperature. Tetramethylsilane at 0.00 ppm or the residual protons of acetone-d_6 at 2.05 ppm were used as internal references. FTIR spectra were recorded on a Nicolet SX20 instrument (courtesy of Nicolet Co.) as acetone solutions in a sodium chloride cell. Computer simulations were obtained with a Commodore

(1) Crutchley, R. J.; Kress, N.; Lever, A. B. P. *J. Am. Chem. Soc.* **1983**, *105*, 1170.
(2) Haga, M.-A.; Dodsworth, E. S.; Eryavec, G.; Seymour, P.; Lever, A. B. P. *Inorg. Chem.*, paper in this issue.
(3) Schilt, A. A. *J. Am. Chem. Soc.* **1963**, *85*, 904.
(4) Peterson, S. H.; Demas, J. N. *J. Am. Chem. Soc.* **1979**, *101*, 6571.
(5) Giordano, P. J.; Bock, C. R.; Wrighton, M. S. *J. Am. Chem. Soc.* **1978**, *100*, 6960.
(6) Giordano, P. J.; Bock, C. R.; Wrighton, M. S.; Interrante, L. V.; Williams, R. F. X. *J. Am. Chem. Soc.* **1977**, *99*, 3187.
(7) Hunziger, M.; Ludi, A. *J. Am. Chem. Soc.* **1977**, *99*, 7370.
(8) Shriver, D. F.; Posner, J. *J. Am. Chem. Soc.* **1966**, *88*, 1672.
(9) Crutchley, R. J.; Lever, A. B. P. *Inorg. Chem.* **1982**, *21*, 2276.
(10) Perrin, D. D.; Armarego, W. L. F.; Perrin, D. R. "Purification of Laboratory Chemicals", 2nd ed.; Pergamon Press: Elmsford, NY, 1980.

0020-1669/85/1324-1906$01.50/0

Table II. Spectroscopic Data in Ethanol/H_2SO_4[a]

concn of H_2SO_4, mol L^{-1}	band II		band I/Ib		band Ia	
	λ_{max}, nm	ϵ	λ_{max}, nm	ϵ	λ_{max}, nm	ϵ
			(a) $Mo(CO)_4bpz$			
0	377	6180	547	7430		
0.5	377	5880	542	6870	sh	
1.0	377	5350	542	6080	630	3340
1.5	377	5270	542	5610	634	4950
2.0	377	4800	546	5080	637	6560
2.5	377	4520	548 (sh)	4850	640	7680
3.0	377	3800	540 (sh)	4800	642	8860
3.5	376 (sh)	3420	522	5980	647	9700
4.0	376 (sh)	2660	522	7410	658	9630
			(b) $W(CO)_4bpz$			
0	380	6670	558	9280		
0.5	379	6470	554	8520	sh	
1.0	379	5980	556	7650	628	6 600
1.5	379	4870	557	6700	631	8 590
2.0	379	4690	560 (sh)	6230	633	10 280
2.5	380	4320	520, 540 (sh)	5720, 6180	634	12 320
3.0	380 (sh)	3510	502, 520 (sh)	6960, 6910	636	12 620
3.5			506	9370	640	12 910
4.0			503	10510	644	11 680

[a] ϵ = molar absorbance (L mol^{-1} cm^{-1}); sh = shoulder. Molar absorbances are not corrected for decomposition. Spectra were recorded immediately after mixing and errors are <2% for 2 M H_2SO_4 and <5% for 4 M H_2SO_4.

Model 8032 microcomputer and an Epson MX80 matrix printer utilized in a plotting mode.

Results and Discussion

The visible absorption spectra of the title species show two bands in the visible region, bands I and II (Tables I and II). These transitions have been studied previously[9,11-16] and are clearly associated with $M(t_{2g}^6) \rightarrow bpz(b_2\pi^*)$ (MLCT I) and $M(t_{2g}^6) \rightarrow bpz(a_2\pi^*)$ (MLCT II), being transitions from the metal d shell to the two lowest lying π^* orbitals of bpz. These are separated by some 7000–8000 cm^{-1}.

The species show marked solvatochromic behavior, with the two MLCT transitions shifting to the blue by up to 3000 cm^{-1} as the dielectric constant of the solvent is increased,[16] behavior similar to the corresponding bipyridine (bpy) complexes.[11,12] There is indeed a simple linear correlation between the shifts of the MLCT transitions in $M(CO)_4(bpy)$ with solvent and those of the complexes under study here.[16] The presence of the two peripheral nitrogen atoms, absent in the bipyridine species, was expected to cause deviations in the linear relationship between the two series, when acidic solvents were considered.

As far as glacial acetic acid and trichloroacetic acid (in ethanol) are concerned, no marked differences were noted and presumably protonation does not occur in these media. However, while the addition of mineral acids, HCl, $HClO_4$, and H_2SO_4, to an ethanolic solution of $M(CO)_4(bpy)$ causes only small solvatochromic shifts (to the blue) in the MLCT band energies, addition to $M(CO)_4$-(bpz) causes new bands to be observed.

Solutions of HCl, $HClO_4$, and H_2SO_4 in either water or ethanol cause gradual decomposition of the complexes, as indicated by a decrease in the intensity of the MLCT bands with time. The rate of decomposition increases with increasing acid concentration, being significant within minutes in 4 M acid. We were not able to identify an acid system that was free of decomposition effects. Such decomposition also continues under an inert atmosphere (CO, N_2). Solutions of H_2SO_4 in ethanol were finally chosen for further study of the protonation since the complexes are readily soluble in this solvent, and decomposition is very slow at low acidities (<3 M). Although some esterification must take place in the mixed $EtOH/H_2SO_4$ medium, it does not seem to be a problem for our study, except that the proton concentration will be uncertain.

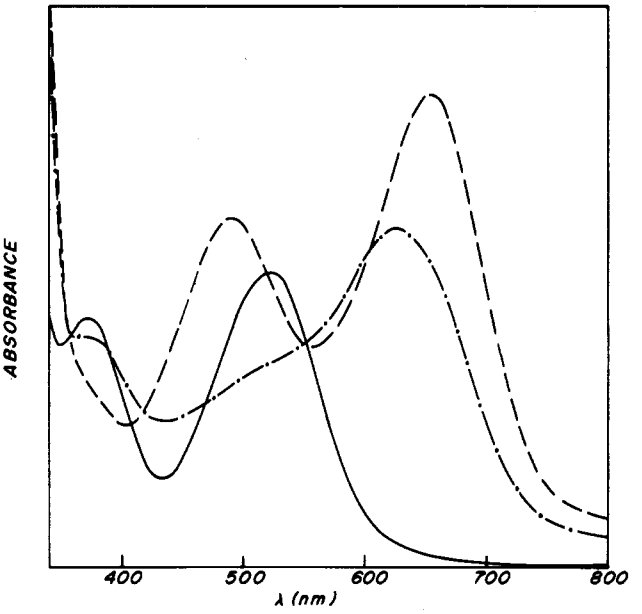

Figure 1. Visible absorption spectra of $Mo(CO)_4bpz$ showing the effect of $Et_2O{\cdot}BF_3$ addition: (—) initial spectrum in acetone; (-·-) predominant species $Mo(CO)_4bpz{\cdot}BF_3$; (- - -) limiting spectrum corresponding (mainly) to

$$Mo(CO)_4bpz{\cdot}BF_3 \xrightleftharpoons{Et_2O{\cdot}BF_3} Mo(CO)_4bpz{\cdot}2BF_3$$

Addition of the Lewis acid, BF_3 (as boron trifluoride etherate), to solutions of the bpz complexes causes spectroscopic effects apparently similar to those of protonation. In both experiments the results for Mo and W complexes are qualitatively the same.

When boron trifluoride etherate is added dropwise to the, initially, pink solution of $M(CO)_4(bpz)$ (M = Mo, W) in acetone, bands I (MLCT I) and II (MLCT II) diminish in intensity and a new band (band Ia) appears at about 618 nm, shifting to lower energy with continued addition of the BF_3. Subsequently, at higher concentrations of the etherate, bands I and II essentially disappear and there remain band Ia and a new band at about 490 nm (band Ib). In pure boron trifluoride etherate as solvent, only bands Ia and Ib are seen, the latter being the more intense. These data

(11) Saito, H.; Fujita, J.; Saito, K. *Bull. Chem. Soc. Jpn.* **1968**, *41*, 863.
(12) Burgess, J. *J. Organomet. Chem.* **1969**, *19*, 218.
(13) Walther, D. *J. Prakt. Chem.* **1974**, *316*, 604.
(14) Manuta, D. M.; Lees, A. J. *Inorg. Chem.* **1983**, *22*, 3825.
(15) Balk, R. W.; Stufkens, D. J.; Oskam, A. *Inorg. Chim. Acta* **1978**, *28*, 133.
(16) Dodsworth, E. S.; Lever, A. B. P.; Eryavec, G., to be submitted for publication in *Inorg. Chem.*

Table III. Carbonyl Stretching Frequencies and Force Constants[a]

	A_1	B_1	A_1	B_2	k_1	k_2	k_i	A_1(calcd)
$Mo(CO)_4bpz$	2020	1919	1896	1851	14.17	15.55	0.34	1890
$+Et_2O{\cdot}BF_3$[b]	2024	1934[c]	1921[c]	1863	14.32	15.72	0.31	1890

[a] Vibrational frequencies cited in cm^{-1}; force constants in mdyn/Å; solvent acetone. [b] Note that the dominant species in the presence of excess $Et_2O{\cdot}BF_3$ is the BF_3 monoadduct; however, some diadduct will be present. [c] The assignments of the 1934- and 1921-cm^{-1} vibrations may be reversed. The reverse assignment leads to k_1 = 14.36, k_2 = 15.60, k_i = 0.35 mdyn/Å; A_1(calcd) = 1891 cm^{-1}.

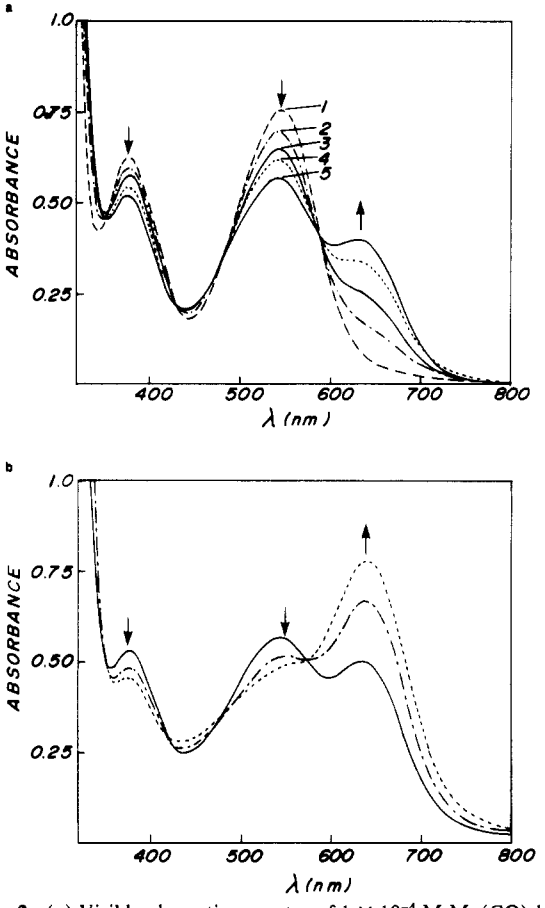

Figure 2. (a) Visible absorption spectra of 1×10^{-4} M $Mo(CO)_4bpz$ in H_2SO_4/ethanol as a function of $[H_2SO_4]$. Curves 1–5 correspond to $[H_2SO_4]$ of 0, 0.5, 0.75, 1.0, and 1.25 mol L^{-1}, respectively. (b) As (a) with $[H_2SO_4]$ = 1.5 M (—), 2.0 M (-·-), and 2.5 M (---).

are summarized in Table I and Figure 1. When the solution is diluted, band Ib diminishes in intensity and bands I and II of the parent species reappear. Thus, the reaction seems quite reversible with little or no decomposition.

Band Ia is associated with MLCT I of the BF_3 monoadduct and band Ib with MLCT I of the BF_3 diadduct. There is no evidence in the data obtained here for bands corresponding to MLCT II appearing in either adduct (at least to the red of the parent transition). The red shifting of band Ia, upon further addition of BF_3 etherate, probably reflects a solvatochromic effect, expected to shift this transition to lower energies as the polar acetone is diluted with the less polar diethyl ether.[14]

Attempts to isolate a solid adduct from reaction of $Et_2O{\cdot}BF_3$ with $Mo(CO)_4bpz$ or $W(CO)_4bpz$ were unsuccessful; reactions of the solids with liquid $Et_2O{\cdot}BF_3$ (at room temperature, in vacuo) produced black oils.

Data for protonation of $Mo(CO)_4bpz$ and $W(CO)_4bpz$ are presented in Table II and typical spectra are shown in Figure 2. As the acidity of the solution is increased, a new peak (band Ia) appears in the spectrum, red shifted with respect to MLCT I. Isosbestic points are observed at 586 and 584 nm for Mo and W species, respectively. Band Ia continues to increase in intensity (and also red shifts slightly), while MLCT I decreases. Above about 1.5 M acid, the isosbestic point is lost, probably because decomposition is beginning to occur. Band I decreases to a shoulder in 2.5 M H_2SO_4. Above this concentration a second new

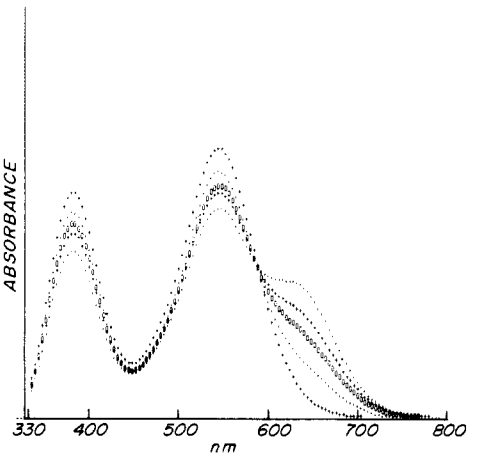

Figure 3. Simulated electronic spectra of $Mo(CO)_4bpz$ and its monoprotonated derivative. The spectra correspond with Figure 2a with the following percentage composition reading from the top spectrum at 377 nm down: (i) 100% parent unprotonated; (ii) 92% parent, 8% monoprotonated; (iii) 86% parent, 14% monoprotonated; (iv) 81.55% parent, 17.95% monoprotonated, 0.5% "diprotonated"; (v) (and lowest at 377 nm) 75% parent, 24% monoprotonated, 1% "diprotonated". The molar absorbances and band widths are as indicated in Table V; Gaussian band shape was simulated.

band (Ib) appears close to the position of MLCT I but significantly blue shifted. This band then increases in intensity relative to band Ia. At acid concentrations greater than 4 M the rate of decomposition of the complex becomes significant relative to the time taken to record the spectrum; thus, the investigation could not be continued.

The effect of acid on MLCT II, the $d \rightarrow a_2\pi^*$ transition, is less easily observed due to its proximity to strong bands in the UV region (bpz $\pi \rightarrow \pi^*$ and $M \rightarrow CO$ MLCT) though it does show a decrease in intensity roughly parallel with MLCT I. No new bands are observed close to MLCT II. This absorption feature disappears altogether from the spectrum in >4 M (Mo) and >3.25 M (W) H_2SO_4.

When acid solutions ($[H^+] < 1$ M) are diluted or neutralized, bands I and II reappear and band Ia diminishes. However, if strong acid solutions, in which band Ib is present, are diluted or neutralized, the reversal is incomplete and the spectra are broad in the region of band I. Furthermore, if a solution in fairly strong acid is monitored with time, band Ib *increases* slightly over short time intervals (minutes) as band Ia decreases. This increase is not associated with growth in band II and cannot therefore reflect an increase in the concentration of the parent complex. Over longer time periods both bands Ia and Ib diminish. We return to this problem below.

Tetracarbonyl diimine complexes of C_{2v} symmetry have four allowed CO stretching modes in their IR spectra: A_1, B_1, A_1, B_2. In $Mo(CO)_4bpz$ the two higher frequency bands correspond primarily to the trans carbonyls and the two lower bands primarily to the cis carbonyls.[9,17,18] FTIR spectra of the CO stretching region and corresponding electronic spectra were recorded for solutions of $Mo(CO)_4bpz$ in acetone and in the presence of varying amounts of $Et_2O{\cdot}BF_3$. Apart from some broadening of the CO bands as BF_3 was added, there was no significant change in the

(17) Adams, D. M. "Metal-Ligand and Related Vibrations"; Edward Arnold: London, 1967; p 101.
(18) Kraihanzel, C. S.; Cotton, F. A. *Inorg. Chem.* **1963**, *2*, 533. Cotton, F. A.; Kraihanzel, C. S. *J. Am. Chem. Soc.* **1962**, *84*, 4432.

Table IV. ^{1}H NMR Spectra of Mo(CO)$_4$bpz and W(CO)$_4$bpz[a]

	H3	H5	H6
Mo(CO)$_4$bpz	10.05	8.90	9.27
+Et$_2$O·BF$_3$ (excess)	10.42	8.97	10.14
W(CO)$_4$bpz	10.08	8.85	9.35
+Et$_2$O·BF$_3$ (excess)	10.41	8.80	10.19

[a] Data in ppm from Me$_4$Si; recorded in acetone-d_6.

spectrum during the growth of band Ia. When there was added a sufficient excess of Et$_2$O·BF$_3$ corresponding to the appearance of band Ib in the electronic spectrum, the energies of all four ν(CO) increased (Table III).

Assignments of the parent carbonyl spectrum (Table III) have already been discussed.[9] As expected for the CO band force constants, k_1 (CO groups trans to diimine) < k_2 (CO groups perpendicular to diimine plane). We anticipate that boron trifluoridation will increase the acceptor power of the diimine and lead to an increase in both k_1 and k_2. The assignment shown in Table III for the BF$_3$ adduct fulfills this expectation, though the fit to the Kraihanzel–Cotton matrices[18] is not quite as good as for the parent species. This poorer fit probably reflects the fact that the dominant species in solution is the monoadduct, which possesses at best C_s symmetry, rather than the C_{2v} symmetry assumed by the theoretical analysis. Other assignments provide even poorer fits to the matrices or result in $k_1 > k_2$. This would imply that bpzBF$_3$ is a better acceptor than CO, which is an improbable result.

Note that these data permit one to derive the ligand effect constants defined by Timney for deducing carbon monoxide stretching force constants.[19] The bpz and BF$_3$ adduct may be compared with bipyridine and CO, as follows:

	cis const, N m^{-1}	trans const, N m^{-1}
bpy	−24	−62
bpz	−13.5	−59
bpzBF$_3$	−5	−52.5
CO	33.5	126.1

The variation is consistent with the ligands becoming better π acceptors in the sequence bpy < bpz < bpzBF$_3$ ≪ CO.

^{1}H NMR spectra were recorded in acetone-d_6 solution and in the presence of an excess of Et$_2$O·BF$_3$ (Table IV). The complex itself shows three resonances in the aromatic region.[9] On addition of Et$_2$O·BF$_3$ the same three resonances are observed, recognizable by their splitting patterns, but H3 and H6 are shifted downfield (H6 shows around twice the shift of H3) while H5 remains at almost the same position. These shifts can be interpreted in terms of a combination of several effects, as discussed by Martin et al.[20] who have recently reported the ^{1}H NMR spectra of a series of substituted pyridines and their BF$_3$ and BBr$_3$ adducts.

The CO stretching frequency data for Mo(CO)$_4$bpz (see above) indicate that the electron density on the metal decreases when the BF$_3$ adduct is formed. This may be due to either weaker σ donation from the bpz or to increased π back-donation to the bpz, either one of which will add to the net deshielding of proton H6. Increased back-donation (and thus a net increase in ring current) seems more probable since this may explain why H3 shifts downfield when H5 does not, H3 being in a stronger field due to the π electrons of both rings.

The NMR data for BF$_3$ addition appear to indicate that only one (symmetric) species is present in solutions containing an excess of Et$_2$O·BF$_3$. Since the reaction is reversible, it is possible that the rate of exchange of BF$_3$ is fast on the NMR scale so that an average signal is seen, due to the equilibrium between the mono- and diadduct BF$_3$ species.

The above results are interpreted in terms of a series of equilibria between the complex and the mono and diadduct species. For example, in the case of protonation

$$M(CO)_4bpz \overset{H^+}{\rightleftharpoons} [M(CO)_4bpzH]^+ \overset{H^+}{\rightleftharpoons} [M(CO)_4bpzH_2]^{2+}$$

Band Ia is attributed to the MLCT transition in the monoprotonated complex. It increases in intensity as the acid concentration is increased and the equilibrium moves to the right, while bands I and II, due to the neutral species, decrease.

Approximate pK_a values may be calculated for the first protonation step where isosbestic points are present in the spectra. Values obtained at 283 K (assuming [H$^+$] = [H$_2$SO$_4$]) are around −0.3 for Mo and +0.1 for W complexes, though there is some variation in the apparent pK_a with acid concentration (due to experimental error and to other equilibria between the acid and solvent). These values are reasonable, lying between those of free bpz (pK_a = 0.45) and [Ru(bpz)$_3$]$^{2+}$ (pK_a = −2.2).[1]. Although bonding to metal(0) might be expected to increase the pK_a of bpz, evidently back-bonding to the CO groups takes most of the M(0) π-electron density.

The molecular orbitals of bipyrazine may be constructed by combining the orbitals of two pyrazine units in and out of phase, resulting in a low-lying π^* orbital of b_2 symmetry and a higher lying π^* orbital of a_2 symmetry. This latter orbital is constructed of the a_u π^* orbital of pyrazine (in D_{2h} symmetry), which possesses a nodal plane through the two nitrogen atoms.[21] It is likely that the dominant contribution to the bipyrazine a_2 π^* state also possesses nodal planes through the nitrogen atoms, providing a partial explanation of the differing effects of the initial protonation (or boron trifluoridation) upon the two MLCT transitions.

In the neutral species, the b_2 π^* orbital is symmetrically delocalized over the whole bipyrazine unit. In the monoprotonated species, this orbital will be stabilized by addition of a proton. A protonated bipyrazine unit may be created by combining pyz with pyzH$^+$. Although the symmetry is now lowered to C_s, two molecular orbitals corresponding to the original b_2 π^* and a_2 π^* of the neutral ligand are still obtained and we continue to use the same labels. The atomic orbital contributions to the molecular orbitals will be such that the pyzH$^+$ moiety will contribute primarily to the lower energy b_2 π^*, while the a_2* state is probably less perturbed and will still be roughly equally delocalized. The state corresponding to band Ia will therefore involve an electron localized mainly in the protonated pyrazine ring. Compare, for example, the red shift observed on protonation of pyrazine in [Ru(NH$_3$)$_5$(pyz)]$^{2+}$.[22] The metal d orbitals are also expected to be stabilized somewhat as the protonated bpz becomes a strong π acceptor (see below). The net red shift then corresponds to the difference in stabilization of the metal and ligand (b_2 π^*) orbitals.

The first nitrogen atom to be protonated in an excited bipyrazine unit is more basic in the excited state than in the ground state, due to the presence of the excited electron, resulting in a red shift of the MLCT transition (Forster).[23] The second excited state (MLCT II) is not a stronger base than the ground state since a red-shifted band does not appear.[23] This is reasonable if the orbital indeed has nodal planes through the nitrogen atoms.

The well-behaved nature of the spectra obtained with Et$_2$O·BF$_3$ and the clean reversibility leave little doubt that band Ib in this experiment corresponds with the BF$_3$ diadduct, M(CO)$_4$(bpz-(BF$_3$)$_2$). This is blue shifted because the presence of one BF$_3$ group, withdrawing electron density from the bpz ligand, will inhibit binding of the second. Thus, the stability constant for binding the second BF$_3$ unit in the excited state (formally bound to Mo(I)) is less than the corresponding value in the ground state (bound to Mo(0)); hence, a blue shift in the Forster scheme.

Band Ib in the higher molarity H$_2$SO$_4$ data is not so readily identified. The presence of one proton in the monoprotonated species will inhibit the binding of the second proton to a greater degree than in the BF$_3$ situation, because of the added positive

(19) Timney, J. A. *Inorg. Chem.* **1979**, *18*, 2502.
(20) Martin, D. R.; Mondal, J. U.; Williams, R. D.; Iwamoto, J. B.; Massey, N. C.; Nuss, D. M.; Scott, P. L. *Inorg. Chim. Acta* **1983**, *70*, 47.
(21) Jorgenson, W. L.; Salem, L. "The Organic Chemists Book of Orbitals"; Academic Press: New York, 1973.
(22) Ford, P.; Rudd, D. P.; Gaunder, R.; Taube, H. *J. Am. Chem. Soc.* **1968**, *90*, 1187.
(23) Ireland, J. F.; Wyatt, P. A. H. *Adv. Phys. Org. Chem.* **1976**, *12*, 131.

Table V. Spectroscopic Parameters

	solvent[a]	transition	energy (ϵ)	band half-width	oscillator strength
$Mo(CO)_4bpz$	A	MLCT I	18 300 (7400)	2880	0.10
		MLCT Ix	20 700 (<2000)[b]	2880[b]	<0.03
		MLCT II	26 530 (6160)	4550	0.13[c]
$Mo(CO)_4bpz$	B	MLCT I	19 230	3260	
		MLCT II	27 130	6200	
$Mo(CO)_4(bpzH)^+$	A (Ia)	MLCT I	15 650 (12 580)	2340	0.13
$Mo(CO)_4(bpzBF_3)$	C (Ia)	MLCT I	15 400	2300	
$Mo(CO)_4(bpz(BF_3)_2)$	C (Ib)	MLCT I	20 400	6000	
$W(CO)_4bpz$	A	MLCT I	17 920 (9280)	2400	0.10
		MLCT II	26 200 (6670)	3800	0.12[c]
$W(CO)_4bpz$	B	MLCT I	18 800	2800	
		MLCT II	27 000		
$W(CO)_4(bpzH)^+$	A (Ia)	MLCT I	15 750	1900	
$W(CO)_4(bpzBF_3)$	C (Ia)	MLCT I	15 630	1850	
$W(CO)_4(bpz(BF_3)_2)$	C (Ib)	MLCT I	20 400	4060	

[a] Key: A = EtOH; B = acetone; C = acetone/ether/BF_3. Data in cm^{-1}. [b] Estimated from deconvoluting MLCT I and MLCT Ix and fitting spectra. [c] Approximate, includes some contribution from UV region.

charge. The second pK_a value for free bipyrazine is −1.35; thus, $K_a(2)/K_a(1) = 63$. This ratio is likely to prevail in the carbonyl complex. With this ratio, $pK_a(2)$ = ca. −2.0 and essentially no (<5%) diprotonated complex would be seen even at the highest acid concentrations used in this study. Thus, either band Ib is extraordinarily intense as MLCT I of the diprotonated species, or it is not associated with the diprotonated species. Since it increases slightly in intensity with time, and band I is not cleanly reproduced upon dilution or neutralization, we suggest that band Ib arises, at least in part, from a decomposition product. The band Ib envelope, however, probably does contain some contribution from the diprotonated species.

Despite this decomposition it is possible to obtain further useful information from the electronic spectra of the protonated species.

The molecular orbital analysis of this system has been disscussed previously.[15,24] The low symmetry (C_{2v}) causes complete loss of degeneracy in the metal d (t_{2g} in O_h) orbitals, resulting in three possible d → π^* transitions under the MLCT I (band I) envelope. In fact, only two of these are electronically allowed and are evident in the spectra recorded in polar solvents as pronounced asymmetry in the band I envelope. In nonpolar solvents where band narrowing occurs, the second transition appears as a weak higher energy shoulder.[15,16,24] The shoulder and band are assigned as the *x*-polarized $a_2(d\pi) \rightarrow b_2(bpz\ \pi^*)$ (band Ix, MLCT Ix) and *z*-polarized $b_2(d\pi) \rightarrow b_2(bpz\ \pi^*)$ (MLCT I) transitions, respectively.[15]

Figure 3 shows a computer simulation of the experimental data in Figure 2a. The Gaussians used are shown for one particular spectrum, in Figure 4. The simulation was obtained in the following manner. The molar intensities and band half-widths of the parent species spectrum are known from the spectrum in ethanol. The existence of isosbestic points at low acidities and the comparatively large separation between the band I and band Ia peaks permit the estimation of the corresponding quantities for the monoprotonated species, assuming the absence of any diprotonated species, a good assumption at low acidity.

The spectra are then created from these data and the calculated percentages of parent and monoprotonated species derived from the experimental spectrum. In a second-order correction of the calculated data, we include a contribution from MLCT Ix and a very small contribution from the decomposition product (band Ib) to achieve a good fit to the experimental data (Figure 3). The molar intensity of MLCT Ix is assumed to be about 25% of that of MLCT I; it cannot be much larger for then it would be revealed as a shoulder. It is assumed to have the same energy difference from MLCT I as observed in nonpolar media. In this approximation, the intensity of band Ib is assumed to be the same as that of band Ia (MLCT I monoprotonated). Its inclusion in the calculated spectrum is necessary to shift the high-energy tail of the band I absorption to higher energy with higher acidity. The band half-width of band Ib was estimated from the high-acidity data. The various parameters used to simulate the spectrum are shown in Table V. The agreement between calculated Gaussian and observed spectra is amazingly good.

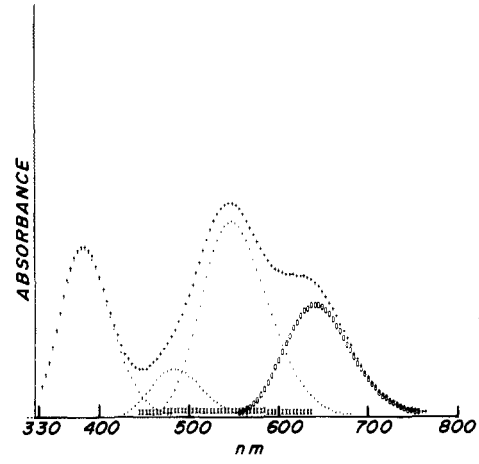

Figure 4. Gaussian construction of the spectrum labeled (v) in Figure 3. The dotted lines correspond with the parent species, the circles to the monoprotonated species, and the crosses to the "diprotonated" species.

Because of the increased decomposition rate, it is not useful to try and simulate the spectra for higher acidities.

The data in Table V merit further consideration. Knowing the molar intensities and band half-widths, it is possible to estimate the oscillator strengths and these are also listed. The MLCT I transition in the monoprotonated species (band Ia) is definitively both narrower and much stronger than the corresponding band in the neutral species. The sharper transition provides evidence that the difference in ground- and excited-state equilibrium distances in this species is smaller than in the parent species. This fact probably reflects a greater degree of covalency in the Mo–N bond with enhanced back-donation because of the greater acceptor power of the now positively charged ligand. The ground state probably has a much greater contribution from valence-bond forms of the type $[Mo^+–bpz^-]$, which is also a description of the MLCT I excited state. Note that since MLCT I is primarily $b_2 \rightarrow b_2^*$, extensive mixing between ground and excited state is permitted by symmetry. A greater mixing of ground and excited state will lead to a smaller difference in bond lengths between these states, as is proposed. It will also lead to greater intensity, since the overlap between ground- and excited-state wavefunctions is obviously increased.[25]

The BF_3 data support the conclusions reached on the basis of protonation. Band Ia, MLCT I in the monoadduct BF_3 species,

(24) Staal, L. H.; Stufkens, D. J.; Oskam, A. *Inorg. Chim. Acta* **1978**, *26*, 255.

(25) Lever, A. B. P. "Inorganic Electronic Spectroscopy", 2nd ed.; Elsevier: Amsterdam, 1968; 1984, Chapter 4.

is also more intense and narrower than MLCT I in the parent species (Table V). Band Ib, MLCT I in the diadduct BF_3 species, is apparently very strong and broad. Its high oscillator strength may be attributed to even greater mixing of metal and bpz orbitals caused by the strongly accepting nature of the two BF_3 groups. The broadness may reflect significant splitting of the d (t_{2g} in O_h) manifold since one of the three d orbitals (b_2) is strongly favored for mixing and hence stabilization relative to the other two.

In conclusion, the protonation and BF_3 data provide evidence for significant mixing between metal and ligand orbitals and the stabilization of a complex whose back-donating character may be very significant.

Acknowledgment. The authors are indebted to Prof. I. M. Walker for useful discussions. We also thank the Natural Sciences and Engineering Research Council of Canada (Ottawa) and the Office of Naval Research (Washington, DC) for financial support. This work is part of a joint ONR Contract with Prof. A. J. Bard.

Registry No. $Mo(CO)_4bpz$, 80907-60-4; $Mo(CO)_4(bpzH)^+$, 95891-49-9; $Mo(CO)_4(bpzBF_3)$, 95891-50-2; $Mo(CO)_4(bpz(BF_3)_2)$, 95891-51-3; $W(CO)_4bpz$, 80925-51-5; $W(CO)_4(bpzH)^+$, 95891-52-4; $W(CO)_4(bpzBF_3)$, 95891-53-5; $W(CO)_4(bpz(BF_3)_2)$, 95891-54-6.

Contribution from the Department of Chemistry and Biochemistry, University of California, Los Angeles, Los Angeles, California 90024

Synthesis and Antibody-Labeling Studies with the *p*-Isothiocyanatobenzene Derivatives of 1,2-Dicarba-*closo*-dodecaborane(12) and the Dodecahydro-7,8-dicarba-*nido*-undecaborate(1−) Ion for Neutron-Capture Therapy of Human Cancer. Crystal and Molecular Structure of $Cs^+[$*nido*-7-(*p*-C_6H_4NCS)-9-I-7,8-$C_2B_9H_{11}]^-$

EUGENE A. MIZUSAWA, MICHAEL R. THOMPSON, and M. FREDERICK HAWTHORNE*

Received January 3, 1985

To investigate the boron-10 labeling of tumor-localizing antibodies, new boron-containing compounds that can be used to conjugate antibody protein have been synthesized. These include the *p*-isothiocyanatophenyl derivatives of 1,2-dicarba-*closo*-dodecaborane(12) and the dodecahydro-7,8-dicarba-*nido*-undecaborate(1−) ion. Antibody-labeling studies using some of these compounds are described. In addition, the cesium salt of the 7-(*p*-isothiocyanatophenyl)-9-iodododecahydro-7,8-dicarba-*nido*-undecaborate(1−) ion, synthesized using formal I^+ that had been generated by the action of *N*-chloro-*p*-toluenesulfonamide on sodium iodide in phosphate buffer, has been characterized by single-crystal, X-ray diffraction methods. The compound crystallized in the monoclinic space group $P2_1/c$, with a = 13.809 (6) Å, b = 12.509 (5) Å, c = 10.601 (3) Å, β = 95.79 (3)°, and Z = 4. Diffraction data to 2θ = 54° (Mo Kα radiation) were collected on a Syntex P$\bar{1}$ diffractometer, and the structure was solved by conventional heavy-atom methods. The final discrepancy indices were R = 0.051 and R_w = 0.061, for 2664 independent reflections. The structure was found to be disordered, with the title compound and its enantiomer occupying the same positions in the unit cell.

Introduction

The potential use of boron-containing compounds in cancer therapy is based on the nuclear property of the boron-10 isotope to absorb thermal neutrons (0.025 eV), releasing an α-particle and recoiling lithium-7 ion with an average total kinetic energy of 2.4 MeV:

$$^{10}_{5}B + {}^{1}_{0}n \rightarrow [^{11}_{5}B] \rightarrow {}^{7}_{3}Li + {}^{4}_{2}He + 2.4\ MeV$$

This type of therapy consists of localizing boron-10 in the tumor mass, followed by external thermal neutron irradiation of the area. The resulting fission fragments, having a range in tissue of less than 10 μm,[1] would deposit the 2.4-MeV energy released in an area confined only to the tumor and to those normal cells immediately surrounding the tumor area.

In 1936,[2] G. L. Locher first proposed the therapeutic possibilities of neutron capture using boron and other elements possessing high-thermal neutron-capture cross sections. In 1940, in vitro studies by Kruger demonstrated the feasibility of boron-10, thermal neutron-capture therapy.[3] In this study, tumor tissues that had been mixed with boric acid and irradiated with thermal neutrons exhibited reduced capacities to be transplanted into mice. Later that same year, Zahl, Cooper, and Dunning, using tumor-bearing mice, claimed a 45% cure or regression due to the boron-10, thermal neutron process.[4] In 1949 Conger and Giles examined the effect of thermal neutrons on plant rootlets.[5] They reported that when boron-10 was introduced, the extent of chromosome damage that was observed was proportional to the amount of boron-10 present.

For normal brain tissue, the entry of foreign chemicals from the bloodstream is prevented by a physiological phenomenon called the blood brain barrier. In the case of most brain tumors, the blood brain barrier is diminished, and on this basis, L. E. Farr in 1951–1952 at the Brookhaven National Laboratory[6-8] and W. H. Sweet 10 years later at the Massachusetts General Hospital[9,10] attempted to treat patients with brain tumors using intravenous boron-10-enriched borax injections followed by thermal neutron irradiation. In both studies, the results were not encouraging, as serious injury to the scalp and blood vessels of the normal brain area was observed.[11]

In Japan, H. Hatanaka has been treating patients with brain tumors since 1972 using boron-10-enriched $Na_2B_{12}H_{11}SH$,[12] and he reports a 33.3% (10/30) 5-year survival with a mean survival time of 36.9 ± 14.8 months.[13] The longest surviving patient is

(1) Tractenberg, M. C.; Kornblith, P. L., Hauptli, J. *Brain Res.* **1972**, *38*, 279.
(2) Locher, G. L. *Am. J. Roentgenol. Radium Ther.* **1936**, *36*, 1.
(3) Kruger, P. G. *Proc. Natl. Acad. Sci. U.S.A.* **1940**, *26*, 181.
(4) Zahl, P. A.; Cooper, F. S.; Dunning, J. A. *Proc. Natl. Acad. Sci. U.S.A.* **1940**, *26*, 591.
(5) Conger, A. D.; Giles, N. H., Jr. *Genetics* **1950**, *35*, 397.
(6) Farr, L. E. *Acta Unio Int. Cancrum* **1955**, *11*, 5.
(7) Farr, L. E.; Sweet, W. H.; Locksley, H. B.; Robertson, J. S. *Trans. Am. Neurol. Assoc.* **1954**, *79*, 110.
(8) Godwin, J. T.; Farr, L. E.; Sweet, W. H.; Robertson, J. S. *Cancer* **1955**, *8*, 601.
(9) Sweet, W. H.; Soloway, A. H.; Brownell, G. L. *Acta Unio Int. Cancrum* **1966**, *16*, 1216.
(10) Sweet, W. H.; Soloway, A. H.; Wright, R. L. *J. Pharmacol. Exp. Ther.* **1962**, *137*, 263.
(11) Brownell, G. L., Murray, B. W.; Sweet, W. H.; Wellum, G. R.; Soloway, A. H. *Proc. Natl. Cancer Conf.* **1973**, *7*, 827.
(12) Hatanaka, H. In "Synthesis and Applications of Isotopically Labeled Compounds"; Duncan, W. P., Susan, A. B., Eds.; Elsevier: Amsterdam, 1983; pp 167–174.
(13) Hatanaka, H. *Proc. First Int. Symp. Neutron Capture Ther.* **1984**, *1*, 384.

0020-1669/85/1324-1911$01.50/0